COMMENTS ON THE FIGURE OF THE MOON BASED ON PRELIMINARY RESULTS FROM LASER ALTIMETRY

W. R. WOLLENHAUPT
NASA Manned Spacecraft Center Houston, Tex., U.S.A.

and

W. L. SJOGREN
Jet Propulsion Laboratory, Pasadena, Calif., U.S.A.

Abstract. Range measurements from the orbiting spacecraft to the lunar surface were made during the Apollo 15 mission using a laser altimeter. The measurements were made in a plane inclined at approximately 26° with respect to the lunar equator. Analysis of measurements made during one complete lunar revolution indicates that the figure of the Moon is very complex. The lunar far side appears to be considerably rougher than the near side in this plane. There appears to be a very large depression on the far side centered at approximately 180° longitude. The near-side maria are depressed with respect to surrounding terrae. These data provide some proof that there is a displacement between the center of figure and the center of mass of the Moon.

1. Introduction

Range measurements from the orbiting Apollo command and service module (CSM) to the lunar surface were obtained during the lunar orbiting phase of the Apollo 15 mission. These data were analyzed to determine a gross estimate of the figure of the Moon in the spacecraft orbit plane. Preliminary results indicate that the Moon has a complex figure in this plane; the lunar far side is considerably rougher than anticipated, and apparently a displacement exists between the center of figure and center of mass of the Moon. In addition, on the far side there appears a very deep depression centered at approximately 180° selenographic longitude (near Van De Graaff).

2. Description of Data

The range measurements were made by using a laser altimeter located in the scientific instrumentation module of the CSM. The altimeter is a ruby laser type which operates in an altitude range of approximately 74–148 km. Resolution of the range measurements is 1 m. A range measurement is obtained every 20 s during automatic mode operation, and once every 16–34 s when the altimeter is operating in conjunction with the mapping camera. During lunar revolutions number 15 and 16, a total of 321 range measurements were made around the entire moon (along a trace of the subvehicle point) with a longitude overlap of approximately 20°. The same features were not measured during the overlap primarily because of the rotation of the Moon. A plot of the ground-track or trace of the sub-vehicle point is presented in Figure 1. Spacecraft altitude during this period was between 95 and 119 k. This paper presents the preliminary results of analyzing these data.

Communication presented at the Conference on Lunar Geophysics, held between October 18–21, 1971, at the Lunar Science Institute in Houston, Texas, U.S.A.

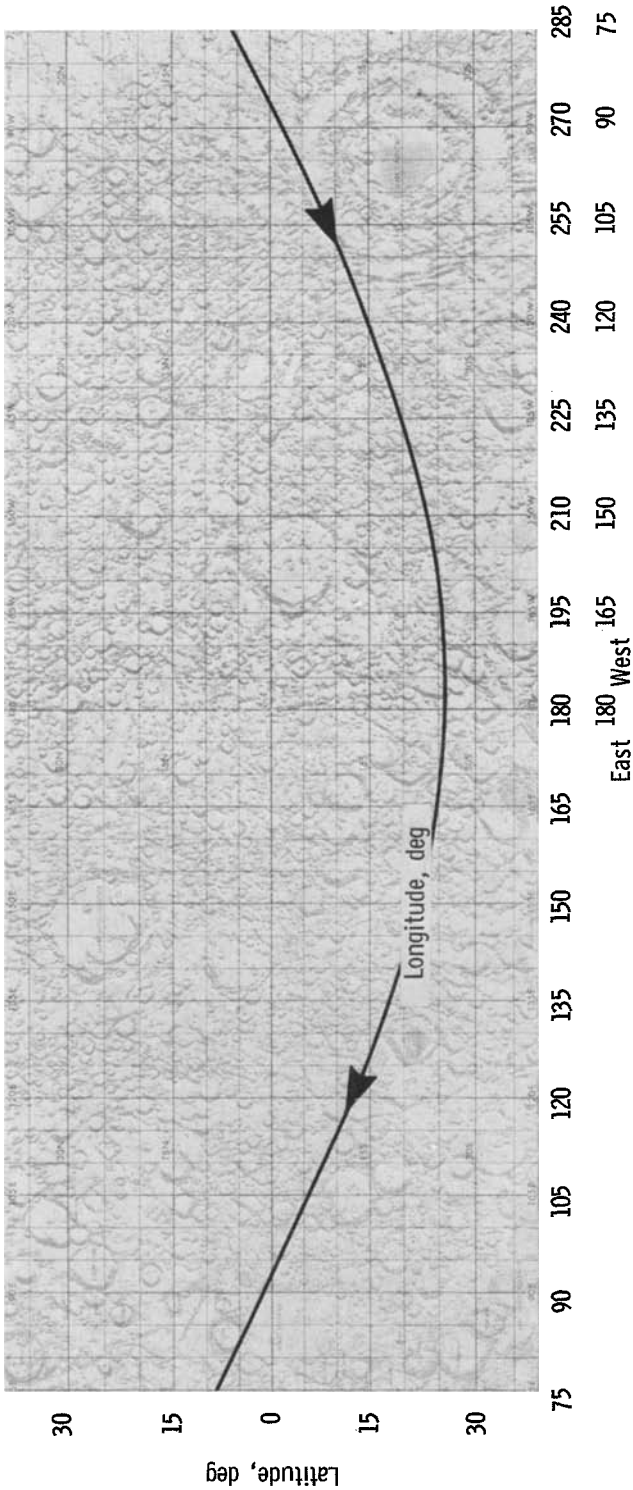

Fig. 1a. Altimeter measurement trace – lunar farside.

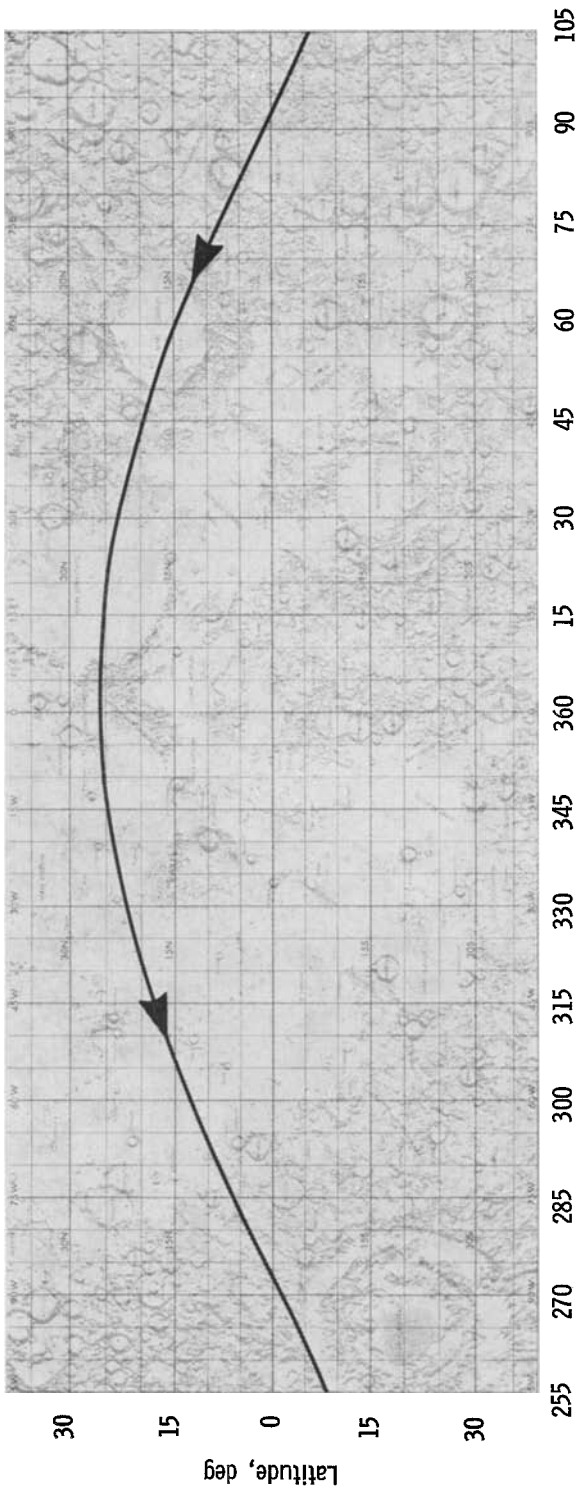

Fig. 1b. Altimeter measurement trace – lunar nearside.

3. Analysis Techniques

In order to interpret the altimeter range measurements, an accurate estimate of the spacecraft position with respect to the Moon at each measurement time is necessary. This is accomplished by use of Doppler frequency shift measurements made by the Manned Space Flight Network (MSFN) radar stations that track the spacecraft whenever it is in line of sight of the station. The location of the tracking stations and the Earth-orbital geometry are such that the spacecraft, when not occulted by the Moon, is in simultaneous view of at least two stations. The Doppler data are processed using a weighted least-squares technique to determine the Moon-centered Cartesian components of the spacecraft orbit at a specified time. This determination is made with respect to center of mass of the Moon. The station observations are corrected for all known systematic errors, such as refraction effects, and timing differences between universal time and ground station time. A five-element spherical harmonic model* is used to describe the lunar gravitational potential for both data processing and trajectory prediction. This model does not completely account for the observed gravitational effect and is the dominant error source in the orbital and prediction computations.

After the spacecraft orbit has been determined, the vehicle position with respect to the center of mass at altimeter measurement times is determined by using Cowell's method of numerical integration to integrate both the equations of motion and variational equations. The estimated altitude above the lunar surface is then computed by assuming that the Moon is a sphere having a radius of 1738 k. The altimeter slant range measurements are then converted to altitudes above the surface by accounting for the altimeter pointing angle deviations from the spacecraft local vertical. This correction has not been applied to the data presented in this paper; therefore, the uncertainties are larger than those expected for the final data reduction. The current uncertainties associated with the selenographic position of the laser altimeter points and the absolute radius values of these points are estimated to be 0.2° for both latitude and longitude and 400 m for radius. The uncertainty associated with the relative altitudes, on the lunar surface, derived from the altimeter measurements is 10 m.

A test of the analysis techniques and of the validity of the altimeter measurements was made by comparing the altimeter-derived radius values with those obtained by independent methods. Radius values were available for three relatively small craters locared in Mare Smythii, Mare Serenitatis, and Palus Putredinis**. The altimeter-derived radius values and the crater values agreed to within 100 m. This can only be considered as a gross test because the laser measurements were not made on exactly the same features.

A small least-squares computer program was then used to fit the above radius devia-

* A lunar gravitational potential model, known as the L-1 model, is used for MSFN orbit determination and trajectory prediction. Coefficients of this model are as follows: $J20 = 2.071\ 08 \times 10^{-4}$; $J30 = -0.21 \times 10^{-4}$; $C22 = 0.207\ 16 \times 10^{-4}$; $C31 = 0.34 \times 10^{-4}$; $C33 = 0.025\ 83 \times 10^{-4}$.

** Locations for these features are discussed in the 'Comments on the Figure of the Moon from Apollo Landmark Tracking', in this publication.

tions from a spherical Moon. It solved for parameters of an ellipsoid and the location of the center of figure. For this analysis, least-squares fits were made to three figures; namely, a sphere, an ellipse, and a constrained ellipsoid. The fit to the ellipse was constrained to the measurement plane, whereas both the spherical and constrained ellipsoid fits were made with respect to the lunar equatorial plane. The fit to the ellipsoid was constrained to a fixed value of 1738.0 km for the z-axis (parallel to the lunar polar axis). Three variations of this type solution were made. Two solutions were obtained using all data, one of which had a 1 km Δz displacement (parallel to the lunar polar axis)*, while the Δz displacement was set equal to zero for the other solution. For the final solution, the data for the large far-side depression were deleted and the Δz displacement was set equal to zero.

4. Discussion of Results

The numerical values for the altimeter measurement sublunar points and the radius deviations from a spherical Moon of 1738 km radius, with the origin at the center of mass, are presented in Table I. The convention used for tabularizing the data was to list the values in chronological order in the direction of spacecraft motion. The altitude profile and the radius deviations from a 1738 km sphere are graphically presented in Figure 2.

The plots in Figure 2 reveal many dramatic details. The most noticeable are the extreme altitude variations on the far side. It can be seen by comparing the altitude profiles that the lunar far side is considerably rougher than the near side in the plane of measurement. Gagarin appears to be a very deep crater with a depth of 6–7 km.

The most intriguing far side feature is what appears, in its gross shape, to be a very large depression whose deepest point is located approximately 180° longitude (near Van De Graaff). It extends approximately 47° in a longitudinal direction, which corresponds roughly to 1400 km on the lunar surface. No comment can be made on the extent of this feature in a latitudinal direction on the basis of these data**. However, analyses of the Zond 6 photographic data have indicated that a very large far-side depression was detected, with essentially the same large shape in a latitudinal direction, at a longitude of approximately $-170°$ to $-180°$†. Their results show that the depression extends in a latitudinal direction from 30 deg south latitude to the south pole. Their calculations indicate that the average depth of the feature, which they refer to as Mare Southwest, is approximately 4.7 km below a best fitting circle. On the lunar near side (Figure 2b) it can be seen that the maria are depressed with respect to surrounding terrae. The deepest depression was measured in Mare Smythii. The ringed maria Smythii,

* The value of 1 km was selected for the Δz offset because it is the presently accepted value of the north-south displacement determined from Earth-based optical observations.

** Additional laser altimeter measurements were made during other lunar revolutions. Unfortunately, the depression was centered near the orbital antinode. This means that as the Moon rotated underneath the spacecraft orbit, very little latitudinal change occurred at this point on the surface.

† Rodionov, B. N. *et al.*: 1971, *Cosmic Res.* **9**, No. 3.

TABLE I

Laser altimeter sublunar points and radius deviations from spherical Moon

Latitude (Deg)	Longitude (Deg)	ΔR (km)	Latitude (Deg)	Longitude (Deg)	ΔR (km)
8.5	291.4	−2.17	−17.6	232.6	3.57
8.0	290.4	−2.26	−17.9	231.5	2.65
7.5	289.2	−1.70	−18.3	230.2	2.88
7.0	288.1	−2.40	−18.7	229.1	2.31
6.5	287.0	−1.55	−19.1	227.9	4.10
6.0	285.9	−2.02	−19.5	226.7	1.91
5.4	284.8	−1.74	−19.9	225.4	2.94
5.0	283.7	−0.34	−20.1	224.2	2.48
4.4	282.6	−1.32	−20.4	223.0	2.58
3.9	281.5	0.17	−20.8	221.8	2.40
3.4	280.4	0.86	−21.1	220.6	2.79
2.9	279.3	−0.76	−21.4	219.4	3.36
2.4	278.2	−0.64	−21.8	218.1	3.41
1.9	277.2	−0.32	−22.0	216.9	1.70
1.3	276.1	0.35	−22.3	215.6	3.38
0.8	275.1	0.42	−22.6	214.4	2.76
0.3	273.9	0.81	−22.9	213.0	2.23
−0.3	272.8	0.01	−23.1	211.8	1.78
−0.9	271.8	0.84	−23.4	210.4	4.01
−1.3	270.7	−0.27	−23.6	209.2	1.64
−1.9	269.6	1.33	−23.8	208.0	0.34
−2.4	268.5	2.45	−24.0	206.7	3.96
−2.9	267.4	2.35	−24.2	205.5	−2.23
−3.4	266.3	1.96	−24.4	204.3	−1.73
−3.9	265.3	0.41	−24.5	203.2	−0.59
−4.4	264.2	4.13	−24.7	201.6	−0.55
−4.9	263.1	1.30	−24.9	200.2	0.70
−5.5	262.0	1.70	−25.1	198.9	−0.52
−6.0	260.9	1.04	−25.2	197.7	−0.82
−6.5	259.8	0.97	−25.3	196.4	−1.27
−7.0	258.7	1.97	−25.4	195.1	−3.04
−7.5	257.6	0.94	−25.5	193.8	−2.62
−8.0	256.5	1.65	−25.6	192.6	−2.29
−8.5	255.4	1.90	−25.7	191.2	−1.86
−9.0	254.3	2.73	−25.8	189.9	−3.31
−9.5	253.2	4.30	−25.8	188.7	−3.83
−10.0	252.1	3.59	−25.8	187.4	−1.20
−10.5	251.0	2.29	−25.9	186.0	−4.40
−10.9	249.9	2.09	−25.9	184.7	−4.86
−11.4	248.8	2.48	−25.9	183.4	−1.13
−11.9	247.6	2.25	−25.9	182.0	−4.62
−12.4	246.5	3.37	−25.9	180.6	Bad data
−12.8	245.3	3.76	−25.8	178.2	−1.82
−13.3	244.2	2.68	−25.8	177.8	−4.17
−13.7	243.1	2.87	−25.7	176.3	−2.14
−14.2	241.9	2.15	−25.6	174.8	−4.86
−14.6	240.8	2.78	−25.6	173.5	−4.69
−15.1	239.6	5.20	−25.5	172.0	−3.93
−15.5	238.4	4.89	−25.4	170.6	−0.12
−15.9	237.3	2.80	−25.3	169.2	0.24
−16.3	236.2	2.73	−25.1	167.8	−2.15
−16.8	235.0	4.49	−24.9	166.4	−1.91
−17.2	233.8	4.73	−24.7	165.0	0.60

Table I (Continued)

Latitude (Deg)	Longitude (Deg)	ΔR (km)	Latitude (Deg)	Longitude (Deg)	ΔR (km)
−24.5	163.6	0.45	−1.8	96.6	−2.18
−24.3	162.2	−2.92	−1.1	95.4	−0.54
−24.1	160.9	1.47	−0.5	94.3	−1.08
−23.9	159.5	−0.90	−0.1	93.2	−3.12
−23.7	158.1	−3.09	0.4	92.1	−4.63
−23.4	156.7	2.21	0.9	91.0	−4.78
−23.2	155.4	2.79	1.5	89.9	−4.90
−22.9	154.1	4.12	2.0	88.8	−4.87
−22.7	152.8	2.38	2.5	87.6	−4.75
−22.4	151.4	−2.35	3.0	86.5	−4.94
−22.1	150.1	−0.91	3.5	85.4	−4.81
−21.8	148.7	−0.68	4.1	84.3	−2.57
−21.5	147.4	−0.35	4.7	83.1	−1.68
−21.2	146.1	0.28	5.2	82.0	−0.98
−20.8	144.9	4.75	5.8	80.8	−4.12
−20.5	143.6	1.78	6.3	79.7	−3.70
−20.1	142.2	0.90	6.9	78.5	−2.07
−19.7	141.0	2.57	7.5	77.3	−2.84
−19.4	139.6	1.44	8.0	76.1	−3.07
−19.0	138.4	2.38	8.5	75.0	−0.68
−18.6	137.3	0.31	9.1	73.8	−0.06
−18.2	135.8	−1.61	9.6	72.6	−1.71
−17.8	134.6	2.48	10.1	71.5	−0.86
−17.4	133.3	1.46	10.6	70.3	−1.07
−17.0	132.1	2.20	11.1	69.1	−3.24
−16.5	130.8	1.46	11.7	67.8	−2.17
−16.1	129.6	2.42	12.2	66.6	−4.34
−15.6	128.4	1.62	12.7	65.5	−3.73
−15.2	127.1	2.09	13.1	64.3	−4.53
−14.7	125.9	1.87	13.6	63.2	−4.67
−14.3	124.7	0.25	14.0	62.0	−4.83
−13.8	123.5	0.38	14.4	60.8	−4.78
−13.3	122.3	0.80	14.9	59.7	−4.82
−12.8	121.1	1.19	15.3	58.5	−4.59
−12.3	119.9	−0.74	15.7	57.4	−4.60
−11.8	118.7	1.18	16.2	56.3	−4.70
−11.4	117.5	3.40	16.6	55.1	−4.69
−10.9	116.3	0.63	17.0	53.9	−4.66
−10.4	115.2	1.11	17.4	52.7	−4.65
−9.9	114.0	1.24	17.8	51.6	−4.29
−9.3	112.8	2.16	18.2	50.4	−4.18
−8.8	111.7	0.46	18.5	49.2	−1.44
−8.3	110.5	−1.00	18.9	48.0	−2.69
−7.8	109.4	−1.22	19.3	46.8	−1.55
−7.2	108.2	0.82	19.6	45.6	−1.31
−6.7	107.0	0.74	19.9	44.4	−1.56
−6.2	105.8	0.57	20.3	43.3	−1.97
−5.6	104.7	2.23	20.6	42.1	−1.78
−5.1	103.6	1.41	20.9	40.9	−4.21
−4.6	102.4	1.01	21.2	39.6	−2.32
−4.0	101.2	1.04	21.5	38.4	−2.33
−3.4	100.1	0.04	21.8	37.1	−2.33
−2.8	98.9	0.15	22.1	35.9	−2.50
−2.3	97.8	−3.52	22.4	34.6	−2.72

Table I (Continued)

Latitude (Deg)	Longitude (Deg)	ΔR (km)	Latitude (Deg)	Longitude (Deg)	ΔR (km)
22.7	33.4	−1.54	20.6	323.2	−1.72
22.9	32.1	−1.90	20.3	322.0	−1.63
23.2	30.8	−1.60	19.9	320.8	−1.77
23.4	29.6	−3.55	19.5	319.6	−1.68
23.6	28.3	−3.88	19.2	318.4	−1.83
23.9	27.0	−3.81	18.8	317.2	−1.82
24.1	25.8	−3.72	18.4	316.0	−1.83
24.3	24.5	−3.57	18.0	314.8	−1.88
24.5	23.2	−3.49	17.6	313.5	−1.85
24.7	21.9	−3.54	17.2	312.2	−1.96
24.8	20.6	−3.34	16.8	311.0	−1.98
24.9	19.4	−3.47	16.4	309.8	−1.93
25.1	17.9	−3.40	16.0	308.6	−1.21
25.2	16.6	−3.42	15.5	307.5	−1.45
25.3	15.3	−3.30	15.2	306.4	−1.41
25.4	14.0	−3.31	14.8	305.4	−1.46
25.5	12.7	−3.22	14.4	304.4	−1.24
25.6	11.4	−3.25	14.0	303.4	−1.59
25.7	10.1	−3.32	13.6	302.4	−1.60
25.8	8.7	−3.22	13.2	301.4	−1.95
25.9	7.4	−2.11	12.8	300.4	−2.09
25.9	6.0	−0.76	12.4	299.5	−2.02
25.9	4.7	0.43	12.0	298.5	−1.97
26.0	3.4	−2.30	11.6	297.6	−1.91
26.0	2.1	−2.61	11.2	296.6	−1.85
26.0	0.8	−2.40	10.8	295.7	−1.96
25.9	359.4	−2.45	10.4	294.8	−1.80
25.9	358.1	−2.43	10.0	293.8	−1.80
25.8	356.8	−2.22	9.6	292.8	−1.84
25.8	355.4	−1.17	9.2	291.9	−1.81
25.7	354.1	−0.50	8.8	291.0	−1.53
25.6	352.8	−2.14	8.3	290.0	−1.36
25.5	351.4	−2.20	7.9	289.1	−0.75
25.4	350.2	−2.72	7.4	288.1	−1.74
25.3	348.8	−2.54	7.0	287.1	−1.38
25.2	347.5	−2.70	6.5	286.2	−0.92
25.0	346.2	−2.74	6.1	285.3	−1.20
24.9	344.9	−2.70	5.7	284.4	−0.32
24.7	343.6	−2.61	5.3	283.4	0.01
24.5	342.3	−2.48	4.9	282.5	−0.54
24.3	341.0	−2.38	4.4	281.5	1.15
24.1	339.7	−2.27	4.0	280.5	1.13
23.9	338.4	−2.26	3.6	279.6	0.34
23.6	337.1	−2.22	3.1	278.7	−0.04
23.4	335.8	−2.07	2.7	277.8	−0.60
23.2	334.5	−1.93	2.2	276.9	0.12
22.9	333.3	−1.83	1.7	275.9	0.21
22.7	332.0	−1.67	1.3	275.0	0.57
22.4	330.8	−1.66	0.8	274.1	1.22
22.1	329.4	−1.57	0.3	273.1	0.32
21.8	328.2	−1.68	−0.1	272.2	0.51
21.5	327.0	−1.67	−0.5	271.3	1.07
21.2	325.8	−1.66	−1.0	270.3	0.49
20.9	324.5	−1.70			

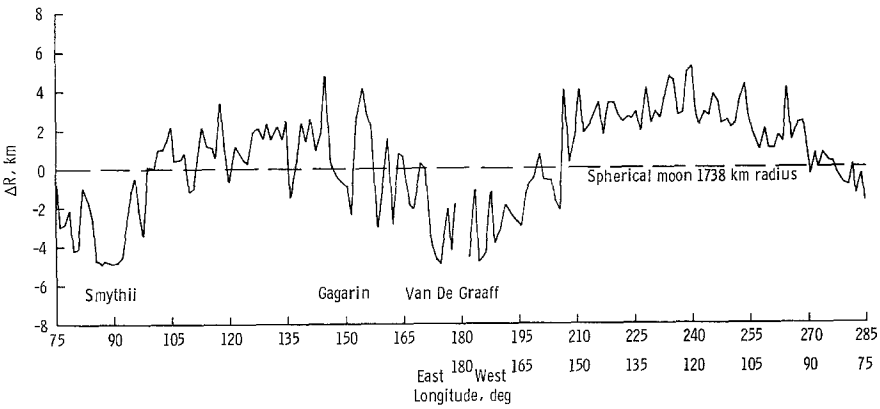

Fig. 2a. Altitude profile and radius deviations from spherical Moon – lunar farside.

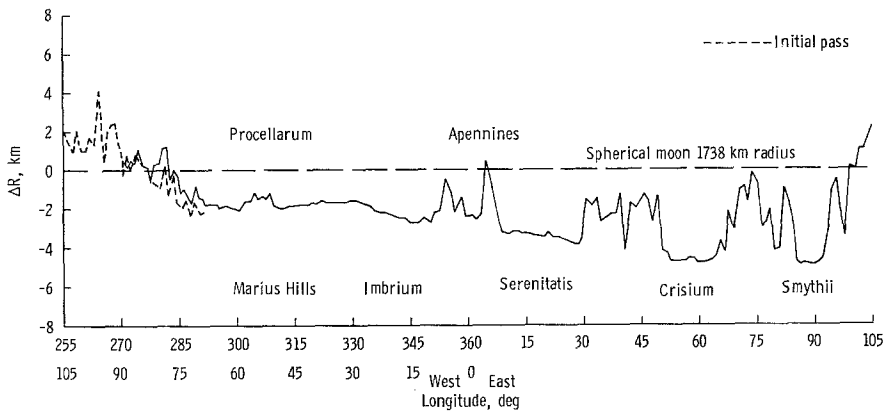

Fig. 2b. Altitude profile and radius deviations from spherical Moon – lunar nearside.

Crisium and Serenitatis are essentially flat. Mare Imbrium appears to slope upward slightly in the direction of Oceanus Procellarum, which in turn is relatively flat. Another interesting detail is the sharp rise in altitude of approximately 3.7 km from Mare Serenitatis to the Apennines.

The results of the least-squares fits to the radius deviations using the technique described in the previous section are summarized in Table II. The best fit sphere had a radius of 1737.1 km, with the center of figure displaced 1.8 k behind and 1.2 km to the left of the center of mass as viewed from the Earth. The ellipse solution yielded the same displacement estimate as the spherical solution. It also indicated a 1.3 km difference between the x-axis parallel to the Earth-Moon line and the y-axis normal to the Earth-Moon line in the plane of measurement, with the y-axis having the largest value. The estimated constrained ellipsoid center of figure to center of mass displacements along the Earth-Moon line (Δx) varied from 1.5–3.8 km, with the center of figure always behind the center of mass. The associated displacements normal to the Earth-Moon

TABLE II

Figure of Moon solutions based on altimeter data

Figure	Principal axes[a], km			Center of mass to center of figure displacements[b], km		
	x	y	z	Δx	Δy	Δz
Sphere	1737.1	1737.1	1737.1	−1.8	−1.2	0[c]
Ellipse	1736.4	1737.7	-	−1.8	−1.2	0[c]
Constrained ellipsoid	1736.1	1737.7	1738.0[c]	−2.0	−1.2	0[c]
Constrained ellipsoid	1736.1	1737.7	1738.0[c]	−1.5	−1.2	−1.0[c]
Constrained ellipsoid[d]	1738.7	1736.5	1738.0[c]	−3.8	−1.9	0[c]

[a] Principal axis orientation: x along Earth-Moon line.
y normal to Earth-Moon line in plane coincident or parallel to lunar equator or orbit plane.
z normal to Earth-Moon line in plane coincident or parallel to lunar polar axis.

[b] Center of Mass (c.m.) to center of figure (c.f.) displacements:
Δx Same orientation as x. Negative means c.f. is behind c.m. when viewing Moon from Earth.
Δy Same orientation as y. Negative means c.f. is to left or west of c.m.
Δz Same orientation as z. Negative means c.f. is below or south of c.m.

[c] Parameter held fixed to indicated value during computations.

[d] Far-side depression data not included in this solution.

line (Δy) in the lunar equatorial plane varied from 1.2–1.9 km for these solutions, with the center of figure always to the left of the center of mass. The estimated x and y-axis values for the two constrained ellipsoid solutions based on all of the data were identical. The only parameter that changed in these solutions was the Δx displacement. The center of figure moved closer to the center of mass for the case which assumed that the center of figure was displaced 1 km below the center of mass; coincident with the lunar polar axis. When the far-side depression data were deleted from the solution, the difference between the x-axis and the y-axis was estimated to be 2.2 km, with the x-axis having the largest value. This is exactly opposite to the results obtained for the ellipse and the other two constrained ellipsoid solutions. In addition, the estimated 3.8 km Δx displacement was much larger than those obtained in previous solutions. The Δy displacement only changed by 0.3 km. This latter case dramatically shows the influence of the far-side depression data on the figure solutions.

5. Concluding Remarks

For the first time, voluminous precision ranging measurements have been made on the lunar far side. These data have shown that the far side may be considerably rougher than previously anticipated, and that, at least in the plane of measurement, it is certainly much rougher than the near side. The far-side data have indicated that a very broad and deep depression extends for approximately 1400 km in a longitudinal direction centered near Van De Graaff. Whether this is a single or a compound feature cannot

be determined from the data used for this paper; nor can its extent in a latitudinal direction be ascertained. However, when the Zond 6 data are considered, it appears that this may be a single feature, at least in a gross sense. A feature of this size could explain a rather large center of figure to center of mass displacement.

This attempts to fit a figure to these data may be nothing more than interesting exercises since the results are certainly not conclusive. However, the data do provide some proof that a center of mass to center of figure displacement exists particularly along the Earth-Moon line. The range of values for this displacement based on these data and the Apollo landmark data (2) indicate that the displacement is somewhere between 1.5 and 3.8 km, with the center of figure behind the center of mass.